Inorg. Chem. **2008**, *47*, 2294−2302

Molecular Architectures for Trimetallic d/f/d Complexes: Magnetic Studies of a $LnCu_2$ Core

Cheri A. Barta, Simon R. Bayly, Paul W. Read, Brian O. Patrick, Robert C. Thompson,* and Chris Orvig*

Department of Chemistry, University of British Columbia, 2036 Main Mall, Vancouver, British Columbia V6T 1Z1, Canada

Received August 13, 2007

Five new trinuclear Cu−Ln−Cu cluster complexes have been prepared by a one-pot reaction using H_3bcn (tris-*N,N′,N″*-(2-hydroxybenzyl)-1,4,7-triazacyclononane) and Ln = La(III), Nd(III), Gd(III), Dy(III), and Yb(III) where the d- and f-block metal ions are in close proximity desirable for magnetic studies. The $[LnCu_2(bcn)_2]ClO_4 \cdot nH_2O$ complexes possess the same stoichiometry as the previously reported $[LnNi_2(bcn)_2]ClO_4 \cdot nH_2O$ and $[LnZn_2(bcn)_2]ClO_4 \cdot nH_2O$ systems. Additionally, the solid state structures of the $LnCu_2$ complexes appear to be isostructural to the $LnNi_2$ and $LnZn_2$ species as determined by their nearly superimposable IR spectra. The similarities in the structures of the $[LnTM_2(bcn)_2]ClO_4 \cdot nH_2O$ series, where TM = Zn(II), Ni(II), and Cu(II), allow for direct comparison of their magnetic exchange. An empirical approach, removing first-order anisotropic contributions determined from the analogous $[LnZn_2(bcn)_2]ClO_4 \cdot nH_2O$ was used to study the d/f/d spin interactions in the $[LnCu_2(bcn)_2]ClO_4 \cdot nH_2O$ complexes. A ferromagnetic exchange was determined where Ln = Gd(III), Dy(III), or Yb(III) and an antiferromagnetic exchange for Ln = Nd(III), identical to the magnetic exchange observed for the $[LnNi_2(bcn)_2]ClO_4 \cdot nH_2O$ complexes. An exchange integral of 3.67 cm^{-1} for the trimetallic $[GdCu_2(bcn)_2]ClO_4 \cdot 3H_2O$ species was determined using a modified spin Hamiltonian. The [Cu(Hbcn)] and the $[Cu_3(Hbcn)_2](ClO_4)_2$ building blocks of the larger coaggregated d/f/d species were also synthesized, and their structures are reported.

Introduction

With the increased interest in new molecular-based magnetic materials, the elucidation of the magnetic interaction between d and f metal ions has become a popular research topic.[1,2] Unfortunately, many obstacles including weak d/f interactions and large anisotropic effects of lanthanide ions (excluding La(III), Gd(III), and Lu(III)) have slowed the progress of research conducted on the magnetic exchange between transition metal (TM) and lanthanide (Ln) ions. Thus, few systematic studies on the structure and magnetic properties of d/f systems have been completed.[3−11]

Most magnetic studies completed on heterometallic d/f complexes have been confined to Gd−Cu systems first introduced by Gatteschi in 1985.[12] Gd(III), a $^8S_{7/2}$ ion, has no first-order orbital momentum in its single-ion ground state. Thus, a rather simple analysis based on the traditional spin-only Hamiltonian exchange model can be amended to quantify the magnetic exchange between the Cu(II) and Gd(III) metal ions.

Several dinuclear Cu−Gd complexes using salen type ligands,[10,11,13−21] in addition to a handful of other isolated

* To whom correspondence should be addressed. E-mail: thompson@chem.ubc.ca (R.C.T.), orvig@chem.ubc.ca (C.O.).

(1) Wernsdorfer, W.; Aliaga-Alcalde, N.; Hendrickson, D. N.; Christou, G. *Nature* **2002**, *416*, 406.
(2) Gatteschi, D.; Sessoli, R. *Angew. Chem., Int. Ed.* **2003**, *42*, 268.
(3) Barta, C. A.; Bayly, S. R.; Read, P. W.; Patrick, B. O.; Thompson, R. C.; Orvig, C. *Inorg. Chem.* **2008**, *47*, 2280–2293.
(4) Kahn, M. L.; Mathoniere, C.; Kahn, O. *Inorg. Chem.* **1999**, *38*, 3692.
(5) Osa, S.; Kido, T.; Matsumoto, N.; Re, N.; Pochaba, A.; Mrozinski, J. *J. Am. Chem. Soc.* **2004**, *126*, 420.
(6) Shiga, T.; Ohba, M.; Ōkawa, H. *Inorg. Chem.* **2004**, *43*, 4435.
(7) Shiga, T.; Ito, N.; Hidaka, A.; Ōkawa, H.; Kitagawa, S.; Ohba, M. *Inorg. Chem.* **2007**, *46*, 3492.
(8) Costes, J.-P.; Dahan, F.; Dupuis, A.; Laurent, J.-P. *Chem.—Eur. J.* **1998**, *4*, 1616.
(9) Kahn, M. L.; Lecante, P.; Verelst, M.; Mathoniere, C.; Kahn, O. *Chem. Mater.* **2000**, *12*, 3073.
(10) Sakamoto, M.; Manseki, K.; Ōkawa, H. *Coord. Chem. Rev.* **2001**, *219–221*, 379.
(11) Benelli, C.; Gatteschi, D. *Chem. Rev.* **2002**, *102*, 2369.
(12) Bencini, A.; Benelli, C.; Caneschi, A.; Carlin, R. L.; Dei, A.; Gatteschi, D. J. *J. Am. Chem. Soc.* **1985**, *107*, 8128.
(13) Ramade, I.; Kahn, O.; Jeannin, Y.; Robert, F. *Inorg. Chem.* **1997**, *36*, 930.

10.1021/ic701613x CCC: $40.75
Published on Web 03/05/2008

Cu−Gd species displaying a variety of geometric demands, have since been synthesized.[11,22–30] The coordination sphere of Cu(II) in these complexes ranges from four-coordinate almost planar, to distorted tetrahedral, to five- or six-coordinate, with a range of intermetallic TM−Ln distances (3.198[13]−3.649[26] Å). Regardless of the geometry around the Cu(II) ion or the proximity of the d/f metal ions, the Cu−Gd complexes exhibited a ferromagnetic exchange[13–15,17,18,20,21] on the order of 2–7 cm^{-1} in all but one case.[16,19] The ferromagnetic exchange is rationalized by either spin polarization effects by Gatteschi et al.[31] or an interaction between the 4f−3d ground-state and the $3d_{Cu} \rightarrow 5d_{Gd}$ charge-transfer configuration suggested by Goodenough[32] and hypothesized by Kahn and Gillon.[33]

Unfortunately, the large first-order orbital contributions of the Ln(III) have complicated the understanding of the magnetic exchange in many Cu−Ln compounds, where Ln ≠ La(III), Gd(III), or Lu(III).[4,8,22,28,34–38] Costes et al. synthesized a Ni−Ln system isostructural to the Cu−Ln species of interest in order to simplify the elucidation of the magnetic exchange between the d/f metal ions.[8] Ni(II) was held in a square planar environment giving rise to a low-spin, diamagnetic state used to determine the non-Curie behavior associated with the f electrons of the Ln(III). Assuming identical crystal-field effects for the two complexes, the magnetic behavior between the d/f metal ions for the Cu−Ln species could be unmasked by removing the first-order orbital contributions of the Ln(III). A similar method was used by Matsumoto whose group synthesized Ni_2Ln_2 systems in order to determine the magnetic exchange in the cyclic cylindrical Cu_2Gd_2 complex.[28] Kahn analyzed the magnetic exchange in the Ln_2Ni_3 and Ln_2Cu_3 polymeric ladder-type compounds by using the analogous Ln_2Zn_3[4,9] where the Zn(II) is d^{10} diamagnetic and, thus, has no magnetic contributions. Ōkawa and co-workers elucidated the magnetic coupling of their 2,6-di(acetoacetyl)pyridine TM−Ln−TM systems, where TM = Cu(II) and Ni(II), utilizing an equivalent Zn−Ln−Zn species.[6,7]

In all the above examples, a ferromagnetic coupling between the Cu(II) and Ln(III), where Ln = Gd(III), Tb(III), and Dy(III) and an antiferromagnetic exchange for Ln = Ce(III), Pr(III), Nd(III), and Sm(III) has been determined. These results follow the theoretical model of Kahn and co-workers predicting that Ln(III) with <7 f electrons will exhibit an antiferromagnetic exchange and with >7 f electrons a ferromagnetic exchange.[21,33] Species with Ho(III), Er(III), and Yb(III) have been shown to exhibit both antiferromagnetic and ferromagnetic interactions, attributed to the differences in the bridging ligand structure between the TM(II) and the Ln(III) (phenolato vs oxamato vs enolate oxygen atoms).

The limited magnetic studies reported for the published d/f complexes, mostly using Cu−Gd systems with very similar Schiff base ligands of similar geometric demands, have kept the field widely unexplored and thus poorly understood. Therefore, it was deemed desirable to design new ligands with different geometric constraints that can afford discrete d/f mixed-metal complexes where the TM(II) and Ln(III) can be varied while maintaining the same core structure.

Utilizing amine phenol ligands previously reported by the Orvig and Wieghardt groups,[39–41] in particular in this study H_3bcn (tris-*N,N′,N″*-(2-hydroxybenzyl)-1,4,7-triazacyclononane),[41] we have synthesized a series of trimetallic Cu−Ln−Cu complexes analogous to the $[LnZn_2(bcn)_2]ClO_4 \cdot nH_2O$ and $[LnNi_2(bcn)_2]ClO_4 \cdot nH_2O$ systems reported in the preceding publication[3] (Scheme 1). An empirical determination of the magnetic interactions of the $[LnCu_2(bcn)_2]ClO_4 \cdot nH_2O$ species was completed using the previously synthesized diamagnetic $[LnZn_2(bcn)_2]ClO_4 \cdot nH_2O$ complexes, similar to the analysis by Costes,[8] Kahn,[4,9] Ōkawa,[6,7] and Matsumoto and co-workers[28] and outlined for the $[LnNi_2(bcn)_2]ClO_4 \cdot nH_2O$ complexes.[3] The synthesis and characterization of these unique trimetallic d/f/d systems where the TM(II) is varied from Ni(II) (studied in the preceding publication)[3] to Cu(II) (investigated herein) will increase the understanding of the necessary requirements to produce desired magnetic properties.

(14) Bencini, A.; Benelli, C.; Caneshi, A.; Dei, A.; Gatteschi, D. *Inorg. Chem.* **1986**, *25*, 572.
(15) Costes, J.-P.; Dahan, F.; Dupuis, A. *Inorg. Chem.* **2000**, *39*, 165.
(16) Costes, J.-P.; Dahan, F.; Dupuis, A. *Inorg. Chem.* **2000**, *39*, 5994.
(17) Costes, J.-P.; Dahan, F.; Dupuis, A.; Laurent, J.-P. *Inorg. Chem.* **1997**, *36*, 3429.
(18) Costes, J.-P.; Dahan, F.; Dupuis, A.; Laurent, J.-P. *Inorg. Chem.* **1996**, *35*, 2400.
(19) Costes, J.-P.; Dahan, F.; Dupuis, A.; Laurent, J.-P. *Inorg. Chem.* **2000**, *39*, 169.
(20) Costes, J.-P.; Novitchi, G.; Shova, S.; Dahan, F.; Donnadieu, B.; Tuchagues, J.-P. *Inorg. Chem.* **2004**, *43*, 7792.
(21) Andruh, M.; Ramade, I.; Codjovi, E.; Guillou, O.; Kahn, O.; Trombe, J. C. *J. Am. Chem. Soc.* **1993**, *115*, 1822.
(22) Stemmler, A. J.; Kampf, J. W.; Kirk, M. L.; Atasi, B. H.; Pecoraro, V. L. *Inorg. Chem.* **1999**, *38*, 2807.
(23) Benelli, C.; Caneschi, A.; Fabretti, A. C.; Gatteschi, D.; Pardi, L. *Inorg. Chem.* **1990**, *29*, 4153.
(24) Gao, S.; Yang, Y.; Xu, G. *J. Alloys Compd.* **1995**, *225*, 234.
(25) Winpenny, R. E. P. *Chem. Soc. Rev.* **1998**, *27*, 447.
(26) Shiga, T.; Ohba, M.; Ōkawa, H. *Inorg. Chem. Commun.* **2003**, *6*, 15.
(27) Ghoerghe, R.; Andruh, M.; Costes, J.-P.; Donnadieu, B. *Chem. Commun.* **2003**, 2778.
(28) Kido, T.; Ikuta, Y.; Suantsuki, Y.; Ogawa, Y.; Matsumoto, N. *Inorg. Chem.* **2003**, *42*, 398.
(29) Costes, J.-P.; Clemente-Juan, J. M.; Dahan, F.; Milon, J. *Inorg. Chem.* **2004**, *43*, 8200.
(30) Sanz, J. L.; Ruiz, R.; Gleizes, A.; Lloret, F.; Faus, J.; Julve, M.; Borras-Almenar, J. J.; Journaux, Y. *Inorg. Chem.* **1996**, *35*, 7384.
(31) Benelli, G.; Caneschi, A.; Gatteschi, D.; Guillou, O.; Pardi, L. *Inorg. Chem.* **1990**, *29*, 1750.
(32) Goodenough, J. B. *Magnetism and the Chemical Bond*; Interscience: New York, 1963.
(33) Kahn, O.; Guillou, O. *Res. Front. Magnetochem.* **1993**, 179.
(34) He, F.; Tong, M.-L.; Chen, X.-M. *Inorg. Chem.* **2005**, *44*, 559.
(35) Costes, J.-P.; Auchel, M.; Dahan, F.; Peyrou, V.; Shova, S.; Wernsdorfer, W. *Inorg. Chem.* **2006**, *45*, 924.
(36) Osa, S.; Kido, T.; Matsumoto, N.; Re, N.; Pochaba, A.; Mrozinski, J. *J. Am. Chem. Soc.* **2003**, *126*, 420.
(37) Guillou, O.; Oushoorn, R. L.; Kahn, O.; Baubekeur, K.; Batail, P. *Angew. Chem., Int. Ed. Engl.* **1992**, *31*, 626.
(38) Li, Y.-T.; Yan, C.-W.; Zhang, J. *Cryst. Growth Des.* **2002**, *3*, 481.
(39) Bayly, S. R.; Xu, Z.; Patrick, B. O.; Rettig, S. J.; Pink, M.; Thompson, R. C.; Orvig, C. *Inorg. Chem.* **2003**, *42*, 1576.
(40) Xu, Z.; Read, P. W.; Hibbs, D. E.; Hursthouse, M. B.; Malik, K. M. A.; Patrick, B. O.; Rettig, S. J.; Seid, M.; Summers, D. A.; Pink, M.; Thompson, R. C.; Orvig, C. *Inorg. Chem.* **2000**, *39*, 508.
(41) Auerbach, U.; Eckert, U.; Wieghardt, K.; Nuber, B.; Weiss, J. *Inorg. Chem.* **1990**, *29*, 938.

Scheme 1. Synthesis of $[LnCu_2(bcn)_2]^+$, Ln = La(III), Nd(III), Gd(III), Dy(III), and Yb(III).

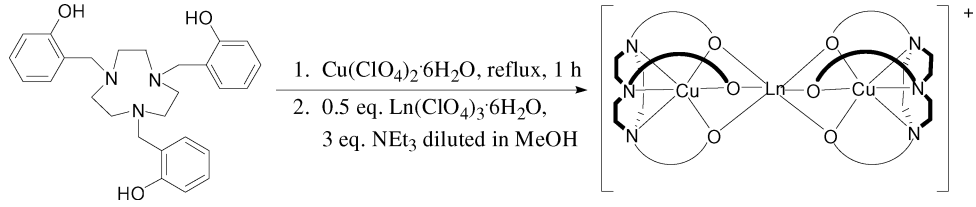

Experimental Section

Materials. Reagents were purchased from commercial sources and used without purification unless otherwise stated. Hydrated Ln(III) perchlorate salts were obtained from Alfa Aesar as 50% (w/w) solutions in water and evaporated to dryness. Methanol and ethanol were dried over activated 4 Å molecular sieves prior to use. Water was deionized (Barnstead D8902 and D8904 Cartridges) and distilled (Hytrex II GX50-9-7/8 and GX100-9-7/8) before use. Yields for the analytically pure compounds were calculated based on the respective metal ion starting material. 1,4,7-Triazacyclononane was synthesized using our literature preparation[3] (adapted from the published[42] procedure).

Caution! *Perchlorate salts are potentially explosive, should be handled with extreme care, and used only in small quantities.*

Physical Measurements. Infrared spectra were recorded as nujol mulls (KBr windows) in the range 4000–500 cm^{-1} on a Mattson Galaxy Series FTIR-5000 spectrophotometer and were referenced to polystyrene (1601 cm^{-1}). Elemental analyses of C, H, and N were performed by Mr. M. Lakha at the University of British Columbia. UV–visible spectra were recorded in methanol using a Hewlett-Packard 8543 diode array spectrophotometer in a 1 cm cuvette. Mass spectra were obtained on a Bruker Esquire Ion Trap (electrospray ionization mass spectrometry, ESI-MS) spectrophotometer. Approximately 1 mg of sample was dissolved in 1 mL of methanol or acetonitrile for +ESI-MS analysis. Room temperature magnetic susceptibilities on the powdered samples of the $[Cu_3(Hbcn)_2](ClO_4)_2 \cdot H_2O$ and $[Cu(Hbcn)] \cdot H_2O$ complexes were measured on a Johnson Matthey MSB-1 balance (solid state) standardized with $CoCl_2 \cdot 6H_2O$ and $CuSO_4 \cdot 5H_2O$. Variable-temperature and applied field magnetic susceptibility measurements on all other $LnTM_2$ complexes were performed on a Quantum Design MPMS XL SQUID magnetometer over the temperature range 2−300 K at 10 000 and 500 G at UBC. Diamagnetic corrections for the constituent atoms used Pascal's constants[43] (6.10×10^{-4} $cm^3\ mol^{-1}$ per mole of complex, plus 3.89×10^{-5} $cm^3\ mol^{-1}$ per water). A specially designed sample holder, as described previously,[44] was used to minimize the background signal. Magnetic susceptibilities were corrected for the background signal generated by the holder.

Synthesis of Complexes. See Table 1 for a list of the $[LnCu_2(bcn)_2]ClO_4 \cdot nH_2O$ complexes prepared and their characterization.

$[Cu(Hbcn)] \cdot H_2O$. To a solution of H_3bcn (27.8 mg, 0.062 mmol) in 20 mL methanol was added $Cu(ClO_4)_2 \cdot 6H_2O$ (22.8 mg, 0.062 mmol). The pale yellow solution became greenish-brown immediately after the addition. The solution was stirred for one hour at RT. The solvent was evaporated to ca. 2 mL. Green crystals formed after slow evaporation of the solvent and were filtered off, washed with cold water, and air-dried to yield 19.5 mg, 62%. MS (+ ES-MS): *m/z* 509 $[TM(HL) + H]^+$. $\mu_{eff} = 1.79\mu_B$. Anal. Calcd. (found) for $C_{27}H_{33}CuN_3O_4$: C, 61.52 (61.80); H, 6.31 (6.34); N, 6.34 (6.31).

Table 1. Analytical Data for $[LnCu_2(bcn)_2]ClO_4 \cdot nH_2O$ Complexes

	% C		% H		% N		+ESI-MS
complex	found	calcd	found	calcd	found	calcd	(*m/z*)
$[LaCu_2(bcn)_2]ClO_4 \cdot 2H_2O$	50.65	50.26	5.06	5.00	7.06	6.51	1155
$[NdCu_2(bcn)_2]ClO_4 \cdot 2H_2O$	50.04	50.05	5.12	4.98	6.72	6.48	1160
$[GdCu_2(bcn)_2]ClO_4 \cdot 3H_2O$	48.19	48.10	5.20	5.01	6.18	6.33	1173
$[DyCu_2(bcn)_2]ClO_4 \cdot H_2O$	48.15	48.26	4.87	5.08	6.43	6.22	1179
$[YbCu_2(bcn)_2]ClO_4 \cdot 2H_2O$	49.11	49.29	5.05	4.87	6.61	6.34	1188

$[Cu_3(Hbcn)_2](ClO_4)_2 \cdot H_2O$. To a solution of H_3bcn (27.9 mg, 0.062 mmol) in methanol was added $Cu(ClO_4)_2 \cdot 6H_2O$ (22.9 mg, 0.062 mmol). The pale yellow solution turned greenish-brown immediately following the addition. The solution was refluxed for 1 h and allowed to cool before the addition of a third equivalent of $Cu(ClO_4)_2 \cdot 6H_2O$ (11.5 mg, 0.03 mmol). The solution was allowed to stir at RT for 30 min before NEt_3 (18.8 mg, 0.186 mmol) was added dropwise. The solvent was evaporated to *ca.* 2 mL affording a light brown precipitate after the additional solvent was slowly evaporated. The powder was filtered off, washed with cold water and air-dried to yield 16.1 mg, 24%. MS (+ESI): *m/z* 1080 $[TM_3L_2+H]^+$. $\mu_{eff} = 2.86\ \mu_B$. Anal. Calcd. (found) for $C_{54}H_{64}Cl_2Cu_3N_6O_{15}$: C, 49.94 (50.28); H, 4.97 (5.08); N 6.47 (6.58).

General Procedure for $[LnCu_2(bcn)_2]ClO_4 \cdot nH_2O$, Ln(III) = La, Nd, Gd, Dy, and Yb. To a solution of $Cu(ClO_4)_2 \cdot 6H_2O$ (92.6 mg, 0.25 mmol) in methanol was added H_3bcn (111.9 mg, 0.25 mmol); the clear solution immediately turned brown. The solution was allowed to reflux while being stirred for 1 h. After the solution was cooled to RT, 1/2 equiv of hydrated $Ln(ClO_4)_3 \cdot 6H_2O$ (68.2–72.4 mg, 0.125 mmol) was added. The brown solution was stirred for an additional 30 min at RT and NEt_3 (75.6 mg, 0.75 mmol) diluted in 5 mL of methanol was added dropwise. After 5 min of stirring, the solution turned green and was immediately filtered through a cotton plug. A pale green powder deposited upon slow evaporation of the solvent. The precipitate was filtered, washed with cold ethanol, and dried in air yielding 40–70%. The ^1H NMR spectra (300 MHz, RT, CD_3OD) was uninformative.

General Procedure for $[LnZn_2(bcn)_2]ClO_4 \cdot nH_2O$, Ln(III) = La, Nd, Gd, Dy, and Yb. The $[LnZn_2(bcn)_2]ClO_4 \cdot nH_2O$ complexes were prepared by the previously described method.[3]

X-ray Structure Determination. The green crystal of the perchlorate salt, isolated by slow evaporation of the solvent from the $[Cu_3(Hbcn)_2](ClO_4)_2$ solution, was mounted on a glass fiber and measurements were taken on a Rigaku/ADSC CCD area detector with graphite monochromated Mo Kα radiation. The structure was processed and corrected for Lorentz and polarization

(42) Richman, J. E.; Atkins, T. J. J. *J. Am. Chem. Soc.* **1974**, *96*, 2268.
(43) Pascal, P. *Chimie Generale*; Masson et Cie: Paris, 1949.
(44) Ehlert, M. K.; Rettig, S. J.; Storr, A.; Thompson, R. C.; Trotter, J. *Can. J. Chem.* **1991**, *69*, 432.

Table 2. Selected Bond Lengths (Å), Intermetallic Distances (Å), and Angles (deg) in $[Cu_3(Hbcn)_2](ClO_4)_2 \cdot 2CH_3OH$

Cu(2)−O(1)	1.939(3)	Cu(1)−O(3)	1.939(3)
Cu(2)−O(3)	1.945(3)	Cu(1)−N(3)	2.007(4)
Cu(2)−Cu(1)	2.9641(5)	Cu(1)−N(1)	2.035(4)
Cu(1)−O(1)	1.931(3)	Cu(1)−N(2)	2.274(3)
O(1)−Cu(1)−O(3)	77.56(11)	N(3)−Cu(1)−N(2)	83.46(14)
N(3)−Cu(1)−N(1)	88.37(16)	N(1)−Cu(1)−N(2)	83.20(13)
O(1)−Cu(1)−N(3)	167.31(14)	Cu(1)−O(1)−Cu(2)	100.00(12)
O(3)−Cu(1)−N(3)	95.71(13)	Cu(1)−O(3)−Cu(2)	99.50(12)
O(1)−Cu(1)−N(1)	94.43(15)	O(1)−Cu(2)−O(1a)	102.77(11)
O(3)−Cu(1)−N(1)	159.84(14)	O(1)−Cu(2)−O(3)	77.23(11)
N(2)−Cu(1)−O(1)	109.14(13)		

effects, and absorption using the d*TREK program.[45] The structure was solved by direct methods[46] and expanded using Fourier techniques.[47] All calculations were performed using the teXsan[48] crystallographic software package of the Molecular Structure Corporation, and SHELXL-97.[49] The nonhydrogen atoms were refined anisotropically. Hydrogen atoms were fixed in calculated positions, but not refined. Selected distances and angles are shown in Table 2, and complete crystallographic data are found in the Supporting Information.

Results and Discussion

$[Cu(Hbcn)] \cdot H_2O$. The Cu(II) building blocks were readily synthesized using one equivalent of $Cu(ClO_4)_2 \cdot 6H_2O$ and H_3bcn in methanol. The EA solved for a stoichiometry of $[Cu(Hbcn)] \cdot H_2O$, confirming the formation of a neutral encapsulated product. A parent peak with 100% relative intensity corresponding to the proton adduct of [Cu(Hbcn)] was also observed in the +ESI-MS spectrum.

A green crystal of [Cu(Hbcn)] was obtained by slow evaporation of the solvent. The crystal structure was found to be analogous to the previously solved [Cu(Hbcn)] species,[41] where three amine nitrogens and two phenolate oxygen atoms from the trisubstituted tacn ligand chelated the Cu(II) ion in a distorted square-based-pyramidal geometry.

$[Cu_3(Hbcn)_2](ClO_4)_2 \cdot H_2O$. Addition of 1 equiv of $Cu(ClO_4)_2 \cdot 6H_2O$ to 2 equiv of deprotonated $[Cu(bcn)]^-$ resulted in a trimetallic transition metal species with the stoichiometry of $[Cu_3(Hbcn)_2](ClO_4)_2 \cdot H_2O$ confirmed by EA. Similar to the previously reported $[Zn_3(bcn)_2]$ and $[Ni_3(bcn)_2] \cdot 2H_2O$ species,[3] only a product peak of 10% relative intensity in the +ESI-MS was observed, suggesting that the stability of the $[Cu_3(Hbcn)_2]^{2+}$ complexes was significantly reduced compared to [Cu(Hbcn)] (the parent peak with 100% relative intensity corresponded to the proton adduct of [Cu(Hbcn)]). In addition, the only significant difference observed in the IR spectra of the monometallic and the trimetallic Cu(II) species was the slightly larger bathochromic shifts of the υ_{C-O} bands attributed to decreased strength in the phenolate oxygen O−TM dative bond from the oxygens bridging an additional Cu(II) ion.

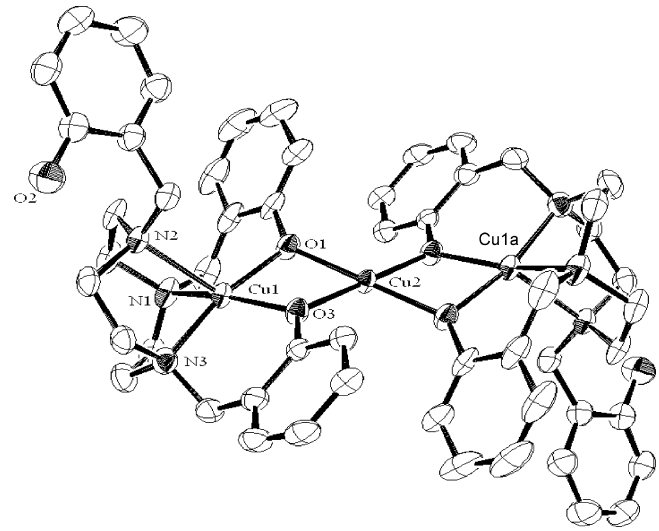

Figure 1. ORTEP diagram of the cation in $[Cu_3(Hbcn)_2](ClO_4)_2 \cdot 2CH_3OH$. Solvent molecules and anions are omitted for clarity, and thermal ellipsoids are drawn at 50% probability.

The crystal structure of $[Cu_3(Hbcn)_2](ClO_4)_2 \cdot 2CH_3OH$ indicates three chelated Cu(II) ions, each 2.96 Å apart (Figure 1). The two terminal Cu(II) centers, related by an inversion center at the bridging Cu(II) ion, are arranged in a distorted square-based-pyramidal environment chelated by three amine nitrogens and two phenolate oxygen atoms. The central Cu(II) is chelated in a square planar geometry by four bridging phenolate donors all in the same plane with an appropriate average bond distance of 1.94 Å.

The O−Cu−O bond angles around the central Cu(II) ion for the two bridging phenolates of the same [Cu(Hbcn)] moiety are appreciably compressed at 77.23°. Alternatively, bond angles between the two capping units are significantly expanded (102.77°), forming a cluster where the alternate bridging O atoms are exactly 180° from each other.

The two terminal Cu(II) ions have characteristic basal Cu−O and Cu−N bond lengths of 1.93 and 2.02 Å, respectively. The basal N−Cu−N, O−Cu−O, and N−Cu−O bond angles are representative of a distorted square-planar system. Deviating from 90° and 180° for regular square planar geometry, the $N_{cis}-Cu-N_{cis}$ and $O_{cis}-Cu-O_{cis}$ angles exhibit an averaged value of 80.51° while an averaged value of 163.58° was observed for the trans N−Cu−O bond. The significantly longer apical Cu−N bond distances of 2.27 Å, similarly seen in the [Cu(Hbcn)] crystal structure, are also characteristic of square-based-pyramidal Cu(II) complexes.[41] An averaged value of 98.46° was observed for the angles between the apical Cu−N bond and the CuN_2O_2 square-planar base with the angles between the $N_{basal}-Cu-N_{apical}$ significantly compressed due to the geometric constraints of the ligand (averaged value of 83.33°). The third phenolic pendant arm, not coordinated to the Cu(II) ion, is bent away from the CuN_3O_2 coordination sphere.

$[LnCu_2(bcn)_2]ClO_4 \cdot nH_2O$. Air-stable complexes of the trinuclear $[LnCu_2(bcn)_2]ClO_4 \cdot nH_2O$ unit (abbreviated as

(45) *D*TREK Area Detector Software*, version 7.11; Molecular Structure Corporation: The Woodlands, TX, 2001.
(46) Altomare, A.; Burla, M. C.; Cammali, G.; Cascarano, M.; Giacovazzo, C.; Guagliardi, A.; Moliterni, A. G. G.; Palidori, G.; Spanga, A. J. *J. Appl. Crystallogr.* **1999**, *32*, 115.
(47) *DIRDIF94 The DIRDIF-94 program system*;, Technical Report of the Crystallography Laboratory, University of Nijmegen: The Netherlands, 1994.
(48) *teXsan Crystal Structure Analysis Package*; Molecular Structure Corporation: The Woodlands, TX, 1985, 1992.
(49) *SHELXL-97*; University of Gottingen: Germany, 1997.

$LnCu_2$) were prepared using protocols adopted from the synthesis of the similar $[LnNi_2(tam)_2]^+$ and $[LnNi_2(trn)_2]^+$ cationic species (Ln = La(III), Nd(III), Gd(III), Dy(III), and Yb(III))[39,40] and the analogous $[LnNi_2(bcn)_2]ClO_4 \cdot nH_2O$ and $[LnZn_2(bcn)_2]ClO_4 \cdot nH_2O$ systems.[3] Spontaneous, self-assembled bicapped structures, where Ln(III) is bridged between the three deprotonated phenolate oxygens from two $[Cu(bcn)]^-$ preorganized ligands, were readily formed upon addition of exactly 6 equiv of triethylamine. The desired d/f/d complexes could not be isolated if a slight excess or shortage of the base was used. The $LnCu_2$ complexes precipitated from their respective reaction mixtures as green powders. Unfortunately, crystals of the desired $LnCu_2$ species were never successfully isolated; however, washing the precipitated solid thoroughly with cold solvents to remove unreacted ligand as well as additional $Ln(ClO_4)_3$ and $Cu(ClO_4)_2$ salts, or other side products, yielded complexes pure by EA. All characterization data, including EA, +ESI-MS, and IR are consistent with the formation of the cationic $[LnCu_2(bcn)_2]^+$ species shown in Table 1.

The elemental analyses for all the lanthanide complexes agreed with the empirical formula $[LnCu_2(bcn)_2]ClO_4 \cdot nH_2O$. The hydrated species observed with other previously synthesized d/f-containing systems are commonly associated with Ln(III) metal ions in order to fulfill their high coordination number preference. +ESI-MS, the primary diagnostic tool for the detection of the cationic d/f/d clusters, gave diagnostic mass spectra with the expected isotopic patterns. The mass spectra were devoid of any other significant peaks besides the parent ion peak for the cationic complex, $[LnCu_2(bcn)_2]^+$.

The coordination geometry around the Cu(II) center appears to change upon coordination to the Ln(III), as monitored by UV–vis. The K-band due to the benzene ring is shifted toward longer wavelengths and a large ligand-to-metal charge transfer band is blue-shifted from 429 to 414 nm upon accommodation of the Ln(III). The d−d transition is significantly red-shifted from 523 nm, as observed in other distorted square planar d^9 Cu(II) ions,[38] to ~670 nm corresponding to an octahedral geometry. The nearly identical weak, broad υ_1 transition at ~670 nm from the $^2E_g \rightarrow {}^2T_{2g}$ in the visible spectra for Cu(II) suggests that the two Cu(II) centers in the bicapped clusters are indistinguishable.[50]

Regardless of the Ln(III) used, the IR spectra for the $[LnCu_2(bcn)_2]ClO_4 \cdot nH_2O$ were nearly superimposable in the 400–3500 cm^{-1} range. In addition, the IR spectra for the $LnCu_2$ species were almost identical to the IR spectra of the previous $[LnNi_2(bcn)_2]ClO_4 \cdot nH_2O$ and $[LnZn_2(bcn)_2]ClO_4 \cdot nH_2O$ species suggesting strongly the formation of isostructural complexes in the solid state. The small <10 cm^{-1} variations in the IR peak frequencies of the various species are attributed to mass differences among the Ln(III) and TM(II) metal ions (Figure 2).

Vibrations for coordinated reaction solvents, specifically methanol (υ_{CH} and υ_{OH} stretches between 2800 and 2700 and 3700–3600 cm^{-1}, respectively) and acetonitrile (υ_2 for CN, υ_3 for HCN, and υ_4 for CC from 2280 to 2320 cm^{-1}) are not observed in the IR.[51] Instead, a broad band at ~3450 cm^{-1} and a narrow band at 600 cm^{-1} attributed to the O−H stretching vibrations suggest the presence of coordinated water molecules used to satisfy the intrinsically large coordination sphere of Ln(III) ions.[52,53] The broadband at ~3150 cm^{-1} is correlated to hydrogen bonded OH groups either between the hydrogen atoms of the coordinated water and/or the oxygen atoms of the ligand chelate, as previously observed in other hydrated Ln(III) complexes.[54] The broadband for the υ_{OH} group is hidden by the coordinated water; however, the absence of υ_{OH} vibrations at 1400 cm^{-1} seen for the $[LnTM_2(bcn)_2]ClO_4 \cdot nH_2O$ species suggest that all phenol groups are deprotonated. The sharp absorption peaks near 1280 and 1100 cm^{-1} for the ν_{C-O} vibration and 1450 cm^{-1} for υ_{C-N} stretching bands are shifted 20–50 cm^{-1} to lower energy with respect to the proligands, evincing normal coordination of the metal ion via the amines and deprotonated phenol oxygens. The υ_{C-O} is slightly more bathochromically shifted due to the phenol oxygen bridging two metals compared to the amine nitrogen coordinated to only one metal ion. In addition, the appearance of new peaks at ~622 cm^{-1} and between 400 and 500 cm^{-1} for ν_{TM-O} and ν_{Ln-O} stretching frequencies, respectively, confirm the complexation of bcn^{3-} to the metal ions.[55–58] The bands at 3000–2860 and 1550 cm^{-1} for the CH and aromatic ring C=C stretching vibrations did not significantly shift upon coordination of the metal ions. In addition, the presence of υ_3 of ClO_4^- at 1068 cm^{-1} for all the complexes suggests the formation of cationic complexes.

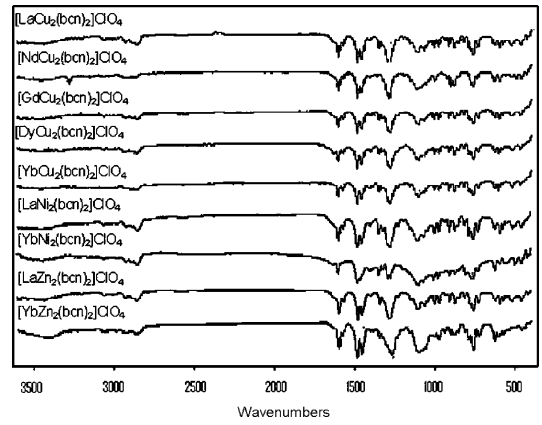

Figure 2. IR spectra of selected $[LnTM_2(bcn)_2]ClO_4 \cdot nH_2O$.

Magnetic Properties. The nearly identical structures of the previously synthesized $[LnTM_2(bcn)_2]ClO_4 \cdot nH_2O$, where

(50) Rafat, F.; Siddiqi, K.; Lutfullah, S. *Synth. React. Inorg. Met.-Org. Chem.* **2004**, *34*, 763.
(51) Bünzli, J.-C. G.; Milicic-Tang, A. *Inorg. Chim. Acta* **1996**, *252*, 221.
(52) Guoxin, T.; Yongjun, Z.; Jingming, X.; Ping, Z. *Inorg. Chem.* **2003**, *42*, 735.
(53) Kameta, N.; Imura, H.; Ohashi, K.; Aoyama, T. *Polyhedron* **2002**, *21*, 805.
(54) Yang, L.; Xu, Y.; Gao, X.; Zhang, S.; Wu, J. *Carbohydr. Res.* **2004**, *339*, 1679.
(55) Comba, P.; Hambley, T. W.; Hitchman, M. A.; Stratemeier, H. *Inorg. Chem.* **1995**, *34*, 3903.
(56) Guillon, H.; Hubert-Pfalzgraf, L. G.; Vaissermann, J. *Eur. J. Inorg. Chem.* **2000**, 1243.
(57) Alyea, E. C.; Malek, A.; Vougioukas, A. E. *Can. J. Chem.* **1981**, *60*, 667.
(58) Brown, L. M.; Mazdiyasni, K. S. *Inorg. Chem.* **1970**, *9*, 2783.

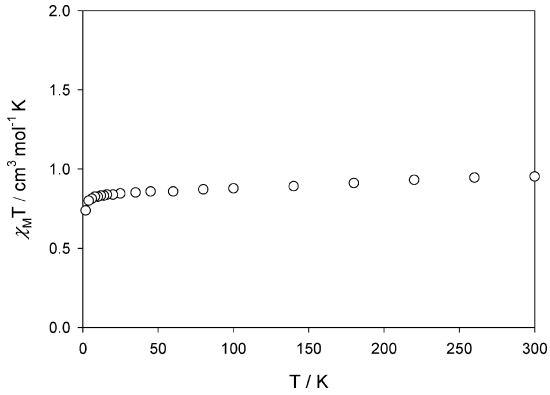

Figure 3. $\chi_M T$ vs T plot of $[LaCu_2(bcn)_2]ClO_4 \cdot 2H_2O$.

TM = Zn(II) and Ni(II), and the $[LnCu_2(bcn)_2]ClO_4 \cdot nH_2O$ species herein allow for the direct comparison of the magnetic properties between the varied d/f/d metal ions, Ln = La(III), Nd(III), Gd(III), Dy(III), and Yb(III). The magnetic susceptibilities of the $[LnCu_2(bcn)_2]ClO_4 \cdot nH_2O$ species were collected on powdered samples using a SQUID magnetometer over a temperature range of 300−2 K. Unfortunately, regression values at high temperatures (>100 K) are only adequate for data taken at the higher magnetic field (10 000 G). Thus, all $\chi_M T$ values reported at RT will be those measured at a magnetic field of 10 000 G. In order to minimize effects from magnetic saturation, $\chi_M T$ values reported herein at <100 K were those obtained using the magnetic field of 500 G. All measurements were corrected for diamagnetism using Pascal's constants.[43] The magnetic susceptibilities of the $[LnZn_2(bcn)_2]ClO_4 \cdot nH_2O$ were previously collected using the same parameters.[3]

The experimental $\chi_M T$ values are compared to the calculated $\chi_M T$ values using eq 1 for two magnetically isolated Cu(II) ions and one Ln(III) ion.

$$\chi_M T = [2g_{Cu}{}^2 S_{Cu}(S_{Cu}+1) + g_J{}^2 J(J+1)]/8 \qquad (1)$$

g is the Landé factor fixed at 2.00, $g_J = 3/2 + [S(S+1) - L(L+1)](2J(J+1))^{-1}$, L is the total orbital angular momentum quantum number, S is the total spin angular momentum quantum number, and J is the total angular momentum quantum number.

The $\chi_M T$ plot for $[LaCu_2(bcn)_2]ClO_4 \cdot 2H_2O$ corresponds well to the expected curve for isolated Cu(II) ions (Figure 3). The experimental $\chi_M T$ of 0.95 cm^3 K mol^{-1} at 300 K is attributed to the two Cu(II) ions with μ_{eff} per Cu(II) = $1.95\mu_\beta$ and $g = 2.26$. Below 10 K, the $\chi_M T$ curve for $LaCu_2$ dips rapidly reaching a minimum of 0.74 cm^3 mol^{-1} K attributed to weak intra- and/or intermolecular antiferromagnetic interactions and/or second order orbital contributions. Nonetheless, the $\chi_M T$ values determined for the two noninteracting Cu(II) ions are in the range of previously reported literature values.[59]

(59) Earnshaw, A. *Introduction to Magnetochemistry*; Academic Press: New York, 1968.

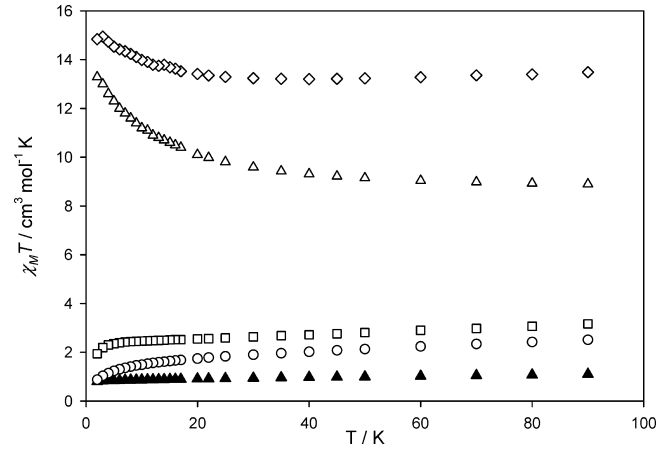

Figure 4. Temperature dependence of $\chi_M T$ for $[LnCu_2(bcn)_2]ClO_4 \cdot nH_2O$ complexes at 500 G: (▲) $LaCu_2$; (○) $NdCu_2$; (△) $GdCu_2$; (◇) $DyCu_2$; (□) $YbCu_2$.

Table 3. Observed and Calculated Magnetic Susceptibilities for $[LnCu_2(bcn)_2]ClO_4 \cdot nH_2O$

Ln(III)	ground state	g_J	$\chi_M T_{calcd}$[a]	$\chi_M T_{obsd}$ (RT)	$\chi_M T_{obsd}$ (2K)	$\Delta(\chi_M T)$[b]	sign of $J_{CuLn}(T)$[c]
La	$^1S_0$		0.75	0.97	0.74		
Nd	$^4I_{9/2}$	8/11	2.40	2.58	0.875	0.30	-
Gd	$^8S_{7/2}$	2	8.64	8.80	13.94	5.98	+
Dy	$^6H_{15/2}$	4/3	14.93	15.18	14.84	6.19	+
Yb	$^2S_{7/2}$	8/7	3.33	3.02	1.94	1.25	+

[a] $\chi_M T$ calculated using eq 1. [b] $\Delta(\chi_M T)$ values were obtained using eq 7 at 2 K. [c] The sign of $J_{CuLn}(T)$ was determined after removing both Ln(III) and Cu(II) contributions.

The Bleaney–Bowers equation was used to elucidate any magnetic interactions between the two terminal Cu(II) metal ions of $[LaCu_2(bcn)_2]ClO_4 \cdot 2H_2O$ that may complicate the magnetic data for the other $[LnCu_2(bcn)_2]ClO_4 \cdot nH_2O$ species. Upon fitting the experimental data to the theoretical curve, no significant interaction between the two Cu(II) metal ions was observed. This conclusion was confirmed by the absence of any significant deviation from Curie's Law using the $\chi_M{}^{-1}$ vs T plot.

The temperature dependent $\chi_M T$ plots of the trinuclear $[LnCu_2(bcn)_2]ClO_4 \cdot nH_2O$ complexes are shown in Figure 4. At 300 K, the $\chi_M T$ of the $[LnCu_2(bcn)_2]ClO_4 \cdot nH_2O$, where Ln = Nd(III), Gd(III), Dy(III), and Yb(III) complexes were determined to be 2.58, 8.80, 15.18, and 3.02 cm^3 K mol^{-1}, respectively, closely corresponding to the calculated values (2.40, 8.64, 14.93, and 3.33 cm^3 K mol^{-1} using eq 1, Table 3) expected for three uncoupled metal ions (S_{cu} =1/2; J = 9/2, g_J = 8/11 for Nd(III); J = 7/2, g_J = 2 for Gd(III); J = 15/2, g_J = 4/3 for Dy(III); J = 7/2, g_J = 8/7 for Yb(III); Table 3).

The $\chi_M T$ data for $NdCu_2$ marginally decrease until 20 K where the values more rapidly decrease reaching its lowest $\chi_M T$ value of 0.875 cm^3 K mol^{-1} at 2 K (Figure 4). This value is significantly lower than the calculated value of 2.40 cm^3 K mol^{-1} expected for the two Cu(II) ions (S_{Cu} =1/2) and the one Nd(III) ion (J = 9/2, g_J = 8/11).

An opposite response was observed for $GdCu_2$ and $DyCu_2$, where the $\chi_M T$ values increased dramatically after 50 and 22 K, respectively (Figure 4). A maximum value of 13.94 cm^3 K mol^{-1} for $GdCu_2$ was reached at 2 K, roughly

matching the calculated value originating from the ferromagnetic coupling between two Cu(II) ions and a Gd(III) ion (12.38 cm^3 K mol^{-1}, eq 2).

$$\chi_M T = (g[S_T(S_T+1)]^{1/2}/2.828)^2 \quad (2)$$

$S_T = 2S_{Cu} + S_{Ln}$ ($S_{Cu} = 1/2$, $S_{Gd} = 7/2$ for $[GdCu_2(bcn)_2]ClO_4 \cdot 3H_2O$), and g is the Landé factor ($g = 2$).

The spin-exchange integral of the $[GdCu_2(bcn)_2]ClO_4 \cdot 3H_2O$ complex was analyzed using a spin-only expression described by the spin Hamiltonian in eq 3.

$$\hat{H} = -2J_{CuGd}(S_{Cu1} \cdot S_{Gd} + S_{Cu2} \cdot S_{Gd}) \quad (3)$$

J_{CuGd} is the exchange integral between the adjacent Cu(II)−Gd(III) ions with the two terminal Cu(II) ions assumed to be identical. A positive J integral suggests a ferromagnetic interaction, whereas a negative value is indicative of an antiferromagnetic exchange. The magnetic data of $GdCu_2$ can be interpreted without considering orbital angular momentum contributions and isotropic effects due to the ground-state of Gd(III) ($^8S_{7/2}$, $J = 7/2$, $L = 0$, and $S = 7/2$) having no first-order orbital angular momentum. The experimental data were fit using eq 4, assuming the Cu(II) and Gd(III) share the same Landé factor.

$$\chi_M = \frac{Ng^2\beta^2}{4k(T-\theta)} \times \frac{(165e^{(16J/kT)} + 84e^{(7J/kT)} + 84e^{(9J/kT)} + 35)}{5e^{(16J/kT)} + 4e^{(7J/kT)} + 4e^{(9J/kT)} + 3)} + N_\alpha \quad (4)$$

N is Avogadro's number, β is the Bohr magneton, k is the Boltzmann constant, N_α is the temperature-independent paramagnetism, g is the Landé factor, θ is a correction term for intermolecular magnetic interactions, and χ_M denotes the molecular susceptibility per trinuclear complex. The agreement factor, $R(\chi_M T)$ defined in eq 5 was used to evaluate how well the experimental data fit the theoretical values.

$$R(R\chi_M T) = \left[\sum (\chi_M T_{obsd} - \chi_M T_{calcd})^2 \Big/ \sum (\chi_M T_{obsd})^2\right]^{1/2} \quad (5)$$

The theoretical expression was fitted to the experimental χ_M vs T data using nonlinear least-squares fitting from 300−2 K. The experimental data for $[GdCu_2(bcn)_2]ClO_4 \cdot 3H_2O$ best fit the theoretical curve using $J = 3.67$ cm^{-1}, $g = 2.07$, and $\theta = -0.20$ K, and $N_\alpha = 12 \times 10^{-5}$ cm^3 mol^{-1} with an agreement factor of $R(\chi_M T) = 9.68 \times 10^{-3}$ (calculated using eq 5, Figure 5). The negative value of θ suggests a slight antiferromagnetic interaction between the terminal Cu(II) ions. The positive J value corresponds to a ferromagnetic exchange between the Cu(II)−Gd(III) ions, previously observed in other trimetallic Cu−Gd−Cu systems.

Ōkawa and co-workers used the same modified Van Vleck equation (eq 4) to elucidate the Cu−Gd interaction for their trimetallic Cu_2Gd system with 2,6-di(acetoacetyl)pyridine as the ligand.[6] They determined $J = 1.44$ cm^{-1}, where the Cu(II) is sandwiched between β-diketonate sites (Cu−Cu intermetallic distance = 7.298 Å) and the Gd(III) ion is chelated by the two central 2,6-diacylpyridine sites (Gd−Cu bond length = 3.649 Å). Gatteschi and co-workers used a different

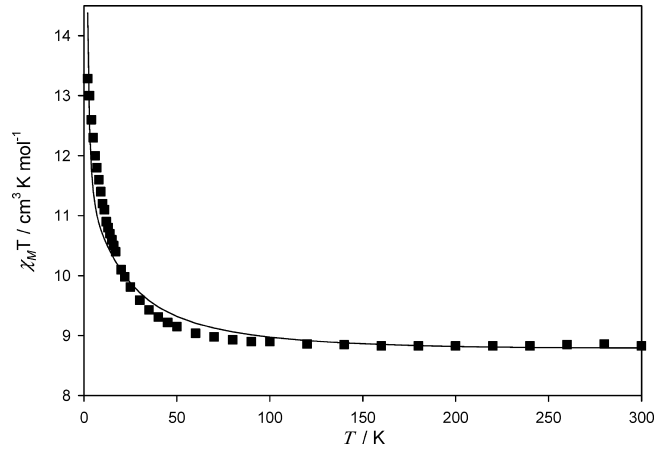

Figure 5. $\chi_M T$ vs T plot for $[GdCu_2(bcn)_2]ClO_4 \cdot 3H_2O$ at 500 G. The solid line represents the theoretical curve calculated using eq 4.

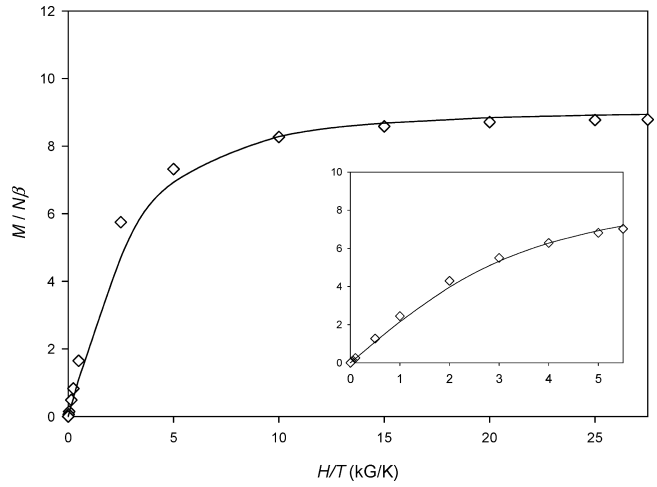

Figure 6. M vs H curve for $[GdCu_2(bcn)_2]ClO_4 \cdot 3H_2O$ at 2 and 10 K (inset). The solid line indicates the theoretical curve from the Brillouin function with $S_T = 9/2$ ($g = 2$).

equation to model the magnetic susceptibility of a trimetallic Cu_2Gd tetradentate Schiff base system;[14] however, their model led to large Cu(II)−Cu(II) antiferromagnetic interaction parameters (Cu−Cu intermetallic distance = 5.41 Å, antiferromagnetic exchange $J = -4.2$ cm^{-1}) that may have skewed the Cu−Gd J value.

The magnetic response, M, at varying fields, H, was used to confirm the ferromagnetic interaction in $[GdCu_2(bcn)_2]ClO_4 \cdot 3H_2O$, where all three metal ions are aligned in parallel with a ground-state of $S_T = 9/2$ (Figure 6). As expected, the experimental M vs H curve closely follows the Brillouin function for $S = 9/2$ suggesting the ferromagnetic ground-state of $S_T = 9/2$, where $S_{Gd} = 7/2$ and $S_{Cu} = 1/2$ for each Cu(II) ion, is significantly populated at 2 K.

$[DyCu_2(bcn)_2]ClO_4 \cdot H_2O$ exhibits a maximum $\chi_M T = 14.94$ cm^3 K mol^{-1} at 3 K, matching the calculated value of 14.93 cm^3 K mol^{-1} using $S_{Cu} = 1/2$ for each Cu(II) ion and $J = 15/2$, $g_J = 4/3$ for the Dy (III) ion. The similar $\chi_M T$ values for the experimental and calculated data of $DyCu_2$ suggest the absence of any magnetic exchange between the metal ions; however, the nearly identical values are probably coincidental, arising from the considerable orbital angular contributions of Dy(III) ($L = 5$) that may offset any observed

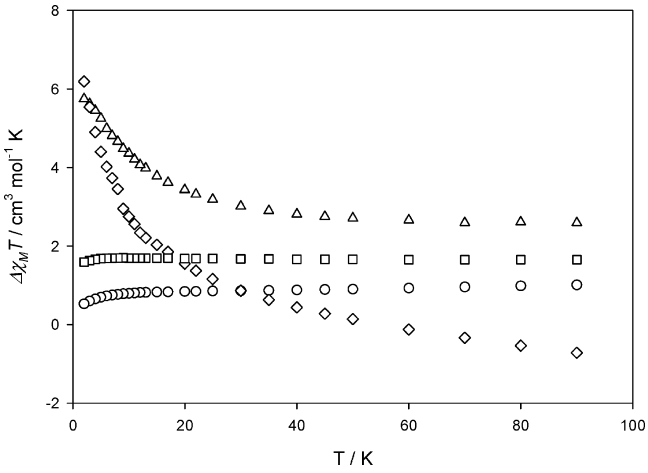

Figure 7. $\Delta\chi_M T$ for $[LnCu_2(bcn)_2]ClO_4 \cdot nH_2O$ complexes: (○) $NdCu_2$; (△) $GdCu_2$; (◇) $DyCu_2$; (□) $YbCu_2$.

ferromagnetic spin exchange between the metal ions. Dy(III) has a large orbital angular momentum with a 16-fold degeneracy of the $^6H_{15/2}$ ground state. The energy gap between the highest and lowest degenerate level is only on the order of a few hundred wavenumbers. Thus, the highest levels are progressively depopulated as the temperature is lowered, leaving only the lowest J sublevel populated at 2 K. This thermal depopulation leads to an inherent decrease of the $\chi_M T$ causing potential deviations from the predicted magnetic behavior (offsetting any possible ferromagnetic interactions between the metal ions).

A modified empirical approach, eq 6, developed by Costes et al.,[8] and used by Kahn,[4,9] Ōkawa,[6,7] and Matsumoto and co-workers[28] can be used to remove intrinsic orbital angular contributions by calculating the difference, $\Delta(\chi_M T)$, between the $\chi_M T$ values for the $LnCu_2$ species and the structurally homologous $LnZn_2$ complexes that may have previously masked any magnetic exchange between the d/f metal ions.

$$\Delta(\chi_M T) = (\chi_M T)_{LnCu_2} - (\chi_M T)_{LnZn_2} = 2(\chi_M T)_{Cu} + J_{CuLn}(T) \quad (6)$$

Ln = La(III), Nd(III), Gd(III), Dy(III), and Yb(III), and $J_{CuLn}(T)$ is related to the nature of the overall exchange interaction between Cu(II) and Ln(III), such that a positive or negative value indicates a ferromagnetic or antiferromagnetic interaction, respectively. Similar crystal field effects are assumed to be operative in both the Cu(II) and Zn(II) complexes due to similarities in their core structures. Intermolecular Cu(II)−Cu(II) magnetic interactions are assumed to be negligible for the d/f/d systems.

After removing the orbital contributions utilizing eq 6, it was found that the $\Delta(\chi_M T)$ values for $GdCu_2$ and $DyCu_2$ increase with decreasing temperatures. In addition, the $\Delta(\chi_M T)$ values at low temperatures (5.98 cm^3 K mol^{-1} at 2 K and 6.19 cm^3 K mol^{-1}at 3 K for $GdCu_2$ and $DyCu_2$, respectively) are significantly higher than the magnetic contribution of 0.75 cm^3 K mol^{-1} for the two isolated Cu(II) ions, indicating a ferromagnetic interaction between the adjacent Cu(II) and Gd(III) or Dy(III) ions (Figure 7). Ōkawa and co-workers determined a $\Delta(\chi_M T)$ value of ∼6 cm^3 K mol^{-1} for their $DyCu_2$ species and a value slightly above 4 for their $GdCu_2$ complexes using an analogous empirical approach,[6] closely matching the ferromagnetic exchange seen for our $[LnCu_2(bcn)_2]ClO_4 \cdot nH_2O$ species. A magnetic exchange at high temperatures, 300 K, was not observed for both the $GdCu_2$ and $DyCu_2$ complexes; the $\Delta(\chi_M T)$ value at 300 K matches only the contributions from the two Cu(II) ions.

Furthermore, the Cu(II) contributions to the $[LnCu_2(bcn)_2]ClO_4 \cdot nH_2O$ systems can be removed using eq 7 to minimize any second-order effects of the Cu(II) ion that may complicate the analysis of the magnetic exchange, thereby leaving only the temperature dependent $J_{CuLn}(T)$ value.

$$J_{CuLn}(T) = (\chi_M T)_{LnCu_2} - (\chi_M T)_{LnZn_2} - (\chi_M T)_{LaCu_2} \quad (7)$$

A negative $J_{CuLn}(T)$ value suggests an antiferromagnetic exchange between metal ions, and a positive value suggests a ferromagnetic exchange. Positive $J_{CuLn}(T)$ values were determined for $GdCu_2$ and $DyCu_2$ (5.14 and 5.35 cm^3 K mol^{-1}, respectively) after subtracting the magnetic data from the analogous $LaCu_2$ species, further suggesting a ferromagnetic interaction between Cu(II), and Gd(III) or Dy(III).

After removing the Nd(III) first-order orbital contributions, $NdCu_2$ exhibited a minimum $\Delta(\chi_M T)$ value of 0.30 cm^3 K mol^{-1}, below the expected magnetic contribution of 0.75 cm^3 K mol^{-1} for two isolated Cu(II) ions, assuming $g = 2$. The decreasing $\Delta(\chi_M T)$ with decreasing temperature and the sustained negative $J_{CuLn}(T)$ value of −0.507 cm^3 K mol^{-1} following the removal of the orbital angular momentum effects from Cu(II) and Ln(III) (using eq 7) further suggests an antiferromagnetic interaction between the Cu(II) and Nd(III) ions; however, the slight decrease in $\chi_M T$ values and the small J value suggests, at best, a very weak magnetic interaction between Cu(II) and Nd(III).

The $\chi_M T$ value for $YbCu_2$ decreases slightly after 20 K and abruptly after 8 K reaching a minimum value of 1.94 cm^3 K mol^{-1} at 2 K, lower than the calculated value of 3.33 cm^3 K mol^{-1}. The dramatic decrease in the $\chi_M T$ values below 8 K may be due to the unquenched angular momentum from Yb(III), masking possible ferromagnetic interactions between the d/f/d metals.

Using the same empirical approach as above, $\Delta(\chi_M T)$ plots for $YbCu_2$ reached a subtle maximum of 1.69 cm^3 K mol^{-1} at 12 K. The value slightly decreases after 12 K, reaching a minimum value of 1.25 cm^3 K mol^{-1} at 2 K. Nonetheless, the $\Delta(\chi_M T)$ value at 2 K is still larger than the magnetic contributions of two Cu(II) ions. If the Cu(II) contributions are removed by eq 7, the empirical $J_{CuLn}(T)$ value is determined to be 0.812 cm^{-1} K mol^{-1} at 12 K or 0.445 cm^{-1} K mol^{-1} at 2 K. The lack of a dramatic decrease in the $\Delta(\chi_M T)$ values and the positive $J_{TMLn}(T)$ value suggests the existence of a weak ferromagnetic exchange previously masked by the first-order orbital contributions of the Ln(III) ion; however, the interaction between the Cu(II) and the Yb(III) cannot be confidently confirmed because of the weak magnetic exchange.

Conclusion

Magnetic interactions in $[LnCu_2(bcn)_2]ClO_4 \cdot nH_2O$ complexes were determined by removing the first-order orbital

contributions of the Ln(III) using an empirical approach similar to the data analysis of Costes and co-workers.[8] $[LnCu_2(bcn)_2]ClO_4 \cdot nH_2O$ displayed ferromagnetic interactions mirroring the $[LnNi_2(bcn)_2]ClO_4 \cdot nH_2O$ complexes where Ln = Gd(III), Dy(III), and Yb(III) and an antiferromagnetic interaction where Ln = Nd(III). To our knowledge, only four trimetallic Cu−Gd−Cu systems (three using tetradentate Cu(II) Schiff base ligands[14,16,60] and one Cu−Ln−Cu species, Ln = La(III), Ce(III), Pr(III), Nd(III), Sm(III), Eu(III), Gd(III), Tb(III), Dy(III), Ho(III), Er(III), Tm(III), and Yb(III) utilizing a 2,6-di(acetoacetyl)pyridine ligand[6]) have been synthesized. Interestingly, these d/f/d complexes displayed similar magnetic properties to the trimetallic Cu−Ln−Cu species discussed herein despite different geometric demands. More importantly, though, these conclusions suggest that the predictions of Kahn et al.[9,33] where a ferromagnetic exchange was observed when using $4f^n$ Ln(III) ions where $n > 7$ and an antiferromagnetic exchange with $n < 7$ are relevant for d/f/d systems regardless of the geometric constraints or the TM(II) used, where TM = Cu(II) or Ni(II).

Acknowledgment. We thank Dr. Cecilia Stevens for her expertise on magnetism and with the UBC SQUID. We acknowledge Discovery Grant support from the Natural Sciences and Engineering Research Council of Canada (R.C.T. and C.O.), a University Graduate Fellowship (C.A.B.) from the University of British Columbia, and a Royal Society Postdoctoral Fellowship (S.R.B.).

Supporting Information Available: Complete tables of crystal parameters and selected IR data. This material is available free of charge via the Internet at http://pubs.acs.org.

IC701613X

(60) Akine, S.; Taniguchi, T.; Nabeshima, T. *Angew. Chem., Int. Ed.* **2002**, *41*, 4670.